Photoreduction of Oxoisoaporphine Dyes by Amines: Transient-Absorption and Semiempirical Quantum-Chemical Studies

Julio R. De la Fuente,* Verónica Neira, Claudio Saitz, Carolina Jullian, and Eduardo Sobarzo-Sanchez

Departamento de Química Orgánica y Fisicoquímica, Facultad de Ciencias Químicas y Farmacéuticas, Universidad de Chile, Casilla 233, Santiago 1, Santiago, Chile

Photoreduction by amines of oxoisoaporphine dyes occurs via a stepwise mechanism of electron−proton−electron transfer that leads to the metastable N-hydrogen oxoisoaporphine anion. During photoreduction that occurs from the triplet manifold of the oxoisoaporphine, a radical ion $\mathbf{A}^{-\bullet}$, a neutral-hydrogenated radical $\mathbf{A\text{-}NH}^{\bullet}$, and the metastable ion $\mathbf{A\text{-}NH}^{-}$ of the oxoisoaporphine are formed. We present time-resolved spectroscopic data and quantum mechanical semiempirical PM3 and ZINDO/S results for the transient species formed during the flash photolysis of oxoisoaporphines in the presence of amines. These calculations reproduce adequately the experimental spectra of the triplet−triplet absorption near 450 nm, and that of neutral hydrogenated radical of the studied oxoisoaporphines centered at 390 nm. A transient absorption observed near 490 nm, for all of the studied systems, was explained by considering the formation of radical ion pair between the radical anion of the oxoisoaporphine, $\mathbf{A}^{-\bullet}$, and the radical cation of the amine, whose ZINDO/S calculated spectra generate the strongest transition near the experimentally observed absorption maximum at 490 nm, supporting the formation of a radical ion pair complex as the first step of the photoreduction.

Introduction

In the photoreduction of many chromophores by electron donors, excited-state quenching by electron transfer from the reductant leads to transient ion-radical pairs, but due to back electron transfer, there are no permanent chemical changes.[1] For some compounds, electron-transfer quenching generates basic radical anions that are easily protonated, and semireduced free radicals accumulate.[2,3] Disproportionation of the radical can generate, among other compounds, stable or metastable products of two-electron reduction or dihydro compounds. Although the photochemistry of these systems is unusual, similar reversible mechanisms involving electron−proton−electron transfer have been reported for reactions of ketones, quinone derivatives, and thioindigo dyes,[2−4] and, more recently, for quinoxalin-2-ones,[5,6] electron-deficient azaarenes,[7] and 2,3-dihydro-oxoisoaporfinas.[8]

It is generally accepted that for some donor−acceptor pairs, excited-state quenching proceeds via sequential transfer of a single electron, **SET**, followed by proton and a second electron transfer, resulting in a net hydride transfer within the quenching complex.[9] This process leads to reactive even-electron ion pairs which are, however, more stable kinetically than ion-radical pairs.[3] The reaction should then be reversible and one or both of the reactants will be recyclable, but examples are relatively rare, because the reversibility of the system depends largely on the thermodynamic stability of these intermediates or metastable products relative to other reaction pathways.[10]

Oxoisoaporphines are a family of oxoisoquinoline-derived alkaloids that have been isolated from *Menispermaceae* as the sole known natural source.[11] In traditional Chinese medicine, the rhizomes of the plants are used as an analgesic; antipyretic and cytotoxic activity has been reported.[12−14] Photoreduction by tertiary amines of synthetic derivatives of oxoisoaporphines,[15−17] **A**, 5,6-dimethoxy-, 5-methoxy-, and 2,3-dihydro-7*H*-dibenzo[*de*,*h*]quinolin-7-one, Scheme 1, in oxygen-free solutions, generates long-lived semireduced metastable photoproducts, $\mathbf{A\text{-}NH}^{-}$, in a stepwise mechanism of electron−proton−electron transfer with a limiting quantum yield approaching 0.1 at high amine concentrations.[8] The $\mathbf{A\text{-}NH}^{-}$ photoproducts revert in the dark to the initial oxoisoaporphine, a process accelerated by oxygen admission to the reaction cell. When photoreduction is performed in the presence of triethylamine, TEA, with any of the studied oxoisoaporphines, among the respective $\mathbf{A\text{-}NH}^{-}$, *N*,*N*-diethyl-1,3-butadienylamine is found as the principal photooxidation product of TEA.[18]

Changes in charge density on methylene carbons C2 and C3 upon conversion of oxoisoaporphines **A3** to the corresponding $\mathbf{A3\text{-}NH}^{-}$ anion, calculated by using PM3 semiempirical quantum method, were consistent with the changes of the ^{1}H NMR chemical shift of the respective protons. The increase in charge density from −0.053 to −0.096 calculated for C2 fits with the upfield shift of the C2 methylene protons from 4.05 to 3.5 ppm. For C3, the decrease in the calculated charge density from −0.074 to −0.053 is in agreement with the downfield shift from 2.86 to 3.15 ppm observed in the ^{1}H NMR spectra;[8] see Scheme 1. Semiempirical quantum mechanical calculations have been used successfully for electronic spectral prediction of neutral molecules, cation-radicals and dications of carotenoids,[19] butadiene derivatives,[20] and, more recently, for phthalocyanines;[21] also we have used this methods to calculate spectroscopic transitions for transient species of 3-phenylquinoxalin-2-ones.[6] In the present work, our interest is to verify how simple semiempirical quantum mechanical calculations can account for the observed UV−visible spectral changes in the photoreduction of the studied oxoisoaporphines.

* Corresponding author. Fax: 56-2-678 2868. E-mail: jrfuente@ciq.uchile.cl.

SCHEME 1

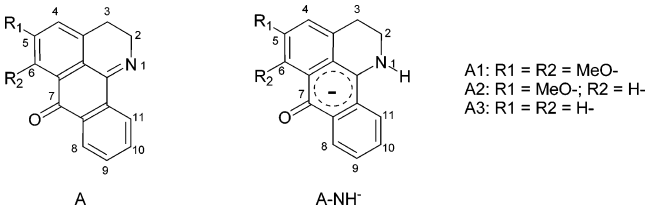

We present a semiempirical quantum mechanical PM3[22] and ZINDO/S[23,24] study of the photoreduced N-hydrogen oxoisoaporphine anion, **A-NH**$^-$, of three synthetic derivatives: 5,6-dimethoxy-, 5-methoxy-, and 2,3-dihydro-7*H*-dibenzo[*de*,*h*]-quinolin-7-one, designated compounds **A1**, **A2**, and **A3**, respectively.

Calculated spectra, employing the PM3 minimized geometries of isolated **A-NH**$^-$ anions, were obtained by using ZINDO/S, and compared with the respective experimental spectra of the semireduced metastable anions. Although these spectra were calculated disregarding any solvent effect, they nicely fit the experimental spectra with respect to the maxima of the absorption bands and the oscillator strength of relative molar absorption intensities at wavelengths over 300 nm. The use of more sophisticated methods, TD-DFT/B3LYP/6-31G*,[25,26] fails to predict the experimental absorption band of **A-NH**$^-$ metastable ion.

We have previously reported[8] that this photoreaction proceeds mainly, if not exclusively, from the triplet manifold of the oxoisoaporphines, through the stepwise mechanism outlined in Scheme 2. The proposed mechanism shows the conversion of oxoisoaporphine **A** into the N-hydrogen anion, **A-NH**$^-$, through the radical anion **A**$^{-\bullet}$, and the neutral radical **A-NH**$^\bullet$. Concomitant with these species, the respective radical cation, $\mathbf{Et_2N^+\cdot CH_2CH_3}$, and the TEA deprotonated radical, $\mathbf{Et_2NC\cdot HCH_3}$, are formed, up to the imine cation final product, $\mathbf{Et_2N^+{=}CHCH_3}$, formed together with **A-NH**$^-$. Imine cation may lead to diethylvinylamine with the final formation of *N*,*N*-diethyl-1,3-butadienylamine with quantum yield near 0.03 or react with H_2O, present in the medium, giving acetaldehyde and diethylamine, as detected by NMR.[8,18]

Results

Semiempirical Quantum Calculations. Semiempirical molecular orbital calculations at PM3 level[22] (HyperChem 6.0 software) were performed to minimize geometries of the product molecules **A-NH**$^-$ of Scheme 2.

The procedure was as follows: for a single molecule of oxoisoaporphine, the geometry was first optimized by using MM+ molecular mechanics[27] followed by unrestricted geometrical optimization at the semiempirical level PM3.

To generate the semireduced species, **A-NH**$^-$, the optimization was performed by adding a hydrogen to the N atom of the optimized structure of **A**, and setting the proper multiplicity and charge, performing the unrestricted geometry optimization for the N-hydrogenated anion **A-NH**$^-$. With optimized geometry of **A-NH**$^-$, electronic spectra were calculated by ZINDO/S, optimized specifically for UV−vis spectroscopy. The calculated spectra were obtained, for each one of the photoreduction products of the studied oxoisoaporphines, with the restricted Hartree−Fock configuration interaction, with orbital criteria using the first 5 unoccupied and 5 occupied MO and weighting overlap factors values of 1.267 and 0.585 used for $\sigma-\sigma$ and $\pi\pi$ overlap respectively.[6,19,20] The results obtained by including more MO (10 + 10) increase the number of absorption lines in the high-energy region below 300 nm, without affecting the spectrally interesting region.

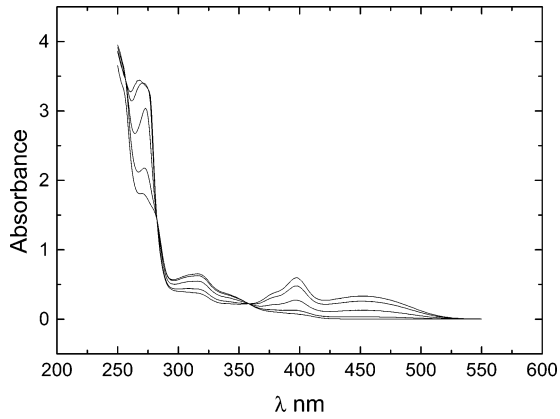

Figure 1. 2,3-Dihydro-oxoisoaporphine **A3** spectra during photoreduction with TEA.

TABLE 1: ZINDO/S/PM3 Calculated Spectra and Experimental Molar Absorption Coefficients for the N-Hydrogen Anion A-NH$^-$

A-NH$^-$	λ nm (calculated)	oscillator strength	λ_{maxima} nm	$\epsilon \times 10^3$ M^{-1} cm^{-1}
A1-NH$^-$	462.9	0.228	468	4.53
	412.9	0.579	405	8.65
	391.0	0.071	386	4.92
	279.3	0.135	278	
	252.0	0.227	268	
A2-NH$^-$	454.8	0.231	450	4.11
	404.5	0.569	394	7.06
	382.0	0.065	374	4.01
	274.8	0.136	284	2.51
	249.9	0.592	270	2.69
A3-NH$^-$	446.3	0.229	452	
	400.5	0.568	398	
	375.3	0.050	378	
	272.0	0.135	342	

The relevant spectroscopically active transitions, at wavelength > 250 nm, calculated for the metastable **A-NH**$^-$ anion of the oxoisoaporphines **A1**, **A2**, and **A3** are summarized in Table 1, together with spectroscopic experimental data.

Although calculations were made for isolated species, all of the calculated spectra show active absorptions compatible with experimental results obtained from photolysis of deoxygenated solutions of the oxoisoporphines in the presence of amines. After a few minutes of photolysis, UV−vis spectra shows significant changes, resulting in the rapid appearance of new absorption bands with isosbestic points at 301 and 378 nm for **A1**; at 307 and 370 nm for **A2**; and at 282 and 358 nm for **A3**, data show in Figure 1 for oxoisoaporphine **A3**. Isosbestic points indicate the clean formation of a single product that has been inequivocally identified as the semireduced N-hydrogenated anion, **A-NH**$^-$, of the respective oxoisoaporphine.[8]

The strong amine absorption at lower wavelength under our experimental conditions precludes comparisons below 300 nm. Good agreement between experimental and calculated photoproduct spectra can be attributed to the small changes in the dipole moment of the states involved, which precludes large solvent-induced Stokes shifts.[28] Figure 2 shows the agreement between calculated ZINDO/S/PM3 and experimental spectra for the oxoisoaporphines anions **A1-NH**$^-$ and **A2-NH**$^-$.

More time-consuming spectral calculations were made for the oxoisoaporphine anion **A3-NH**$^-$, using time-dependent perturbation DFT at B3LYP/6-31G*[25,26] level of theory for the

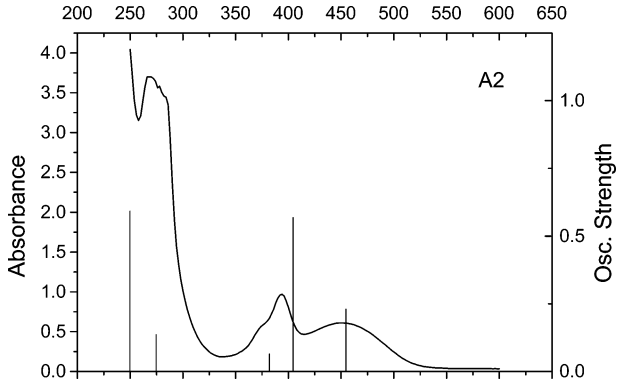

Figure 2. 5-Methoxy-2,3-dihydro-oxoisoaporphine **A2-NH**$^-$ anion, ZINDO/S/PM3 calculated and experimental spectra after complete photoreduction by TEA (Figure 1S for **A1-NH**$^-$).

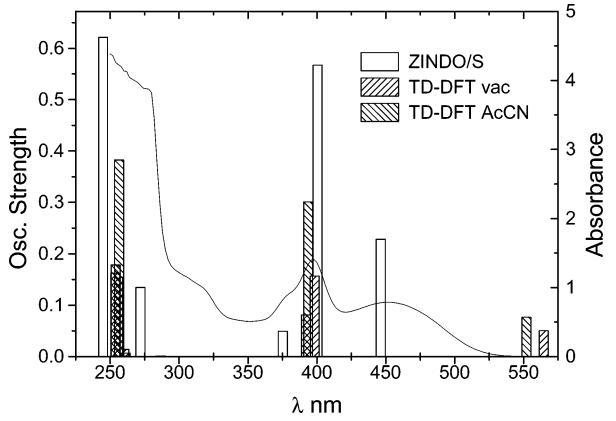

Figure 3. Oxoisoaporphine **A3-NH**$^-$ anion, calculated by ZINDO/S (□); TD-DFT B3LYP/6-31G* vacuum (///); solvated acetonitrile (\\\); and experimental spectra (−) after complete photoreduction by TEA.

isolated molecule and by considering the Tomasi[29] solvation model for acetonitrile with the previously minimized DFT-B3LYP/6-31G* structure of **A3**. The results show discrepancies both with the experimental and with the ZINDO/PM3 calculated spectrum by generating an unobserved absorption near 550 nm, as shown in Figure 3.

Good results for calculated spectra of **A-NH**$^-$, obtained from semiempirical methods, encouraged us to calculate the spectra of the photoreduction intermediates appearing in Scheme 2, that is, the excited triplet state ^{3}**A**, the radical anion of the oxoisoaporphine **A**$^{-\bullet}$, and the neutral radical **A-NH**$^\bullet$, and compare these calculated spectra with the experimental spectra obtained by using laser flash photolysis in the presence of suitable amines.

Calculations were performed on the optimized neutral molecules **A**, for the ground, S_0, and first excited electronic states, singlet S_1 and triplet T_1, by using the ground state PM3 optimized geometry. To obtain the geometry for the relaxed first excited triplet state, a new optimization was made, but now setting the multiplicity of the lowest excited state to 3. This geometrically relaxed triplet was used for the next calculations.

The anion radical **A**$^{-\bullet}$ was generated by setting the proper charge and multiplicity to the relaxed triplet T_1 geometry and was optimized to obtain the geometry and the spectra.

The neutral radical, **A-NH**$^\bullet$, was generated by adding a hydrogen to the N atom of the optimized structure of **A**$^{-\bullet}$, setting the proper multiplicity and charge and then performing the unrestricted geometrical optimization. With optimized geometries of each one of the species mentioned in the preceding paragraphs, electronic spectra were calculated by using ZINDO/S method on the predicted PM3 most stable conformations. Results of these calculations are summarized in Table 2 for the three transient species, where only the spectroscopically active transitions with wavelength greater than 350 nm are considered.

Geometries for the transient intermediates obtained from the optimized ground state of the respective oxoisoaporphine by setting the proper charge and multiplicity and performing the unrestricted PM3 geometrical optimization were nearly identical to those obtained by the procedure described in preceding paragraphs, without significant changes in the ZINDO/S calculated spectra.

SCHEME 2

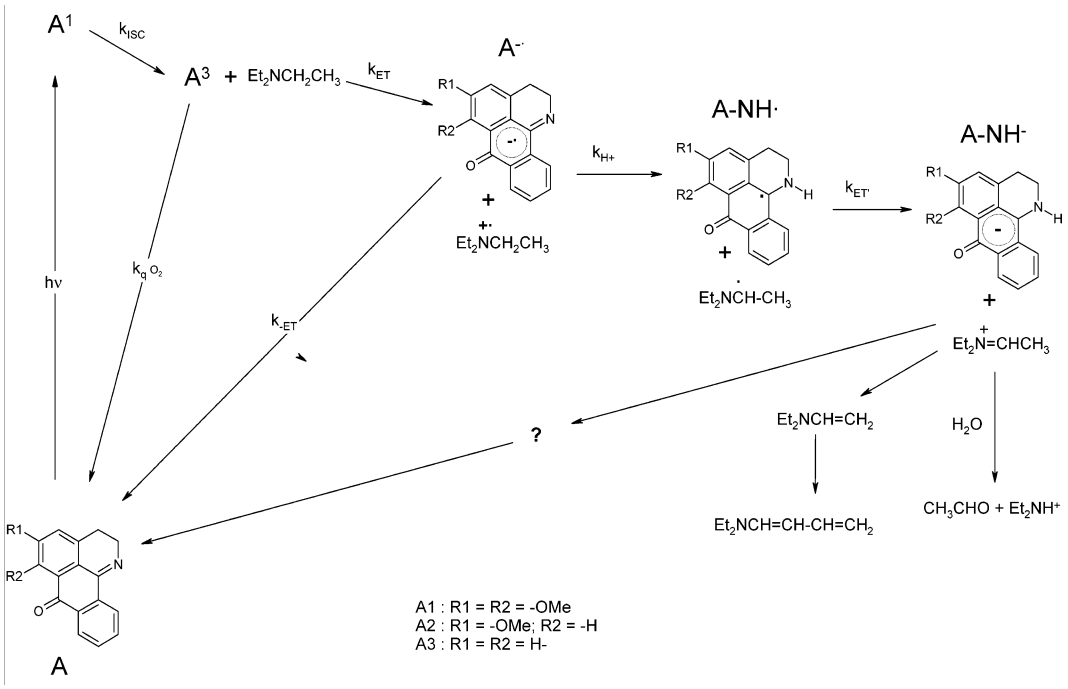

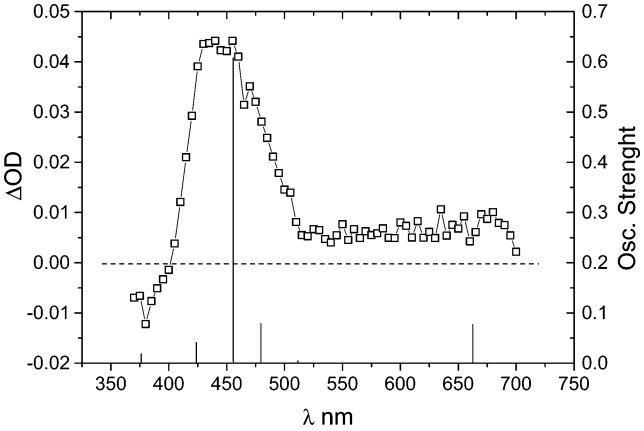

Figure 4. Triplet−triplet absorption spectra of 5,6-dimethoxy-2,3-dihydro-oxoisoaporphine, taken 0.5 μs after laser pulse.

TABLE 2: ZINDO/S/PM3 Calculated Spectra for the Transient Species; Excited Triplet State ^{3}A, Radical Anion A$^{-\bullet}$, and the Neutral N-Hydrogen Radical A-NH$^\bullet$ of 2,3-Dihydro-oxoisoaporphine (Table 1S for A1 and A2)

transient species	^{3}A	A$^{-\bullet}$	A-NH$^\bullet$
	868.2 (0.050)	860.8 (0.050)	538.0 (0.075)
	655.2 (0.006)	616.0 (0.212)	497.3 (0.002)
	585.3 (0.031)	441.4 (0.032)	478.0 (0.033)
	495.1 (0.103)	439.0 (0.001)	416.6 (0.012)
λ nm (osc. strength)	421.4 (0.605)	385.1 (0.051)	384.5 (0.005)
	416.5 (0.037)	361.3 (0.065)	376.9 (0.020)
	371.1 (0.015)	343.2 (0.136)	362.0 (0.157)
			350.1 (0.003)
			340.1 (0.282)
			312.5 (0.099)

Transient Spectroscopy. The transient absorption spectra of the three oxoisoaporphines in nitrogen purged acetonitrile solutions show absorption bands with maximum at 440 nm and a shoulder at 475 nm for **A1**, and maxima at 470 and 450 nm for oxoisoaporphines **A2** and **A3**, respectively. All of the transient spectra show ground-state depletion in the overlapped spectral range below 400 nm. These absorptions have monoexponential decays with lifetimes of about 50 ± 2 and 70 ± 1.5 μs, for oxoisoaporphine **A2** and **A3**, respectively, and a much more shorter lifetime for **A1** near 1.6 ± 0.3 μs. These signals disappear in oxygenated solutions and can be clearly assigned to the triplet excited species ^{3}**A**; see transient spectra in Figure 4 for 5,6-dimethoxy-2,3-dihydro-oxoisoaporphine, **A1**, together with the ZINDO/S calculated transition for the respective triplet and Figure 2S for **A2** and **A3**. Triplet quantum yields, Φ^T, of 0.38, 0.42, and 0.55 for **A1**, **A2**, and **A3**, respectively, were measured by energy transfer to β-carotene, as explained in the Experimental Section.

A good agreement between experimental and calculated spectra for the T−T absorption of the dimethoxy-oxoisoaporphine **A1**, that reproduce the maximum near 450 nm and the shoulder at 475 nm, was found. Although the fit between experimental and calculated T−T absorption spectra for **A3** and **A2** was not so good, the more intense calculated transitions were close to the experimental maximum with less than 30 nm of difference, reproducing the main features of experimental spectra.

In the presence of amines, significant spectral changes occur concomitant with the change in decay profiles from monoexponential to multiexponential with a long-lived residual absorption that remains when amine concentrations are increased.

When non-hydrogen donating amines such as 2,2,6,6-tetramethylpiperidine, TMP, or DABCO were used as electron donors

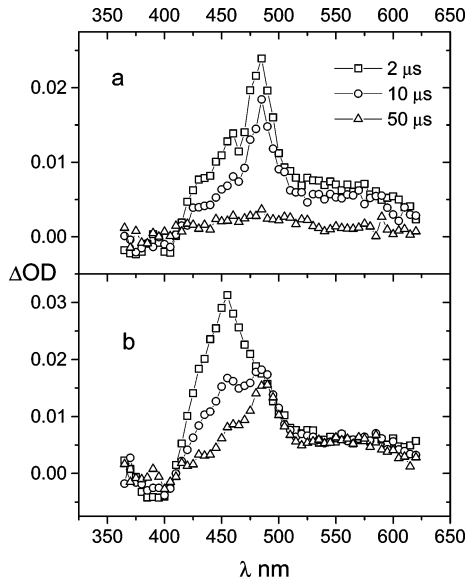

Figure 5. Transient spectra obtained for 2,3-dihydro-oxoisoaporphine, **A3** in the presence of: (a) DABCO 0.1 mM and (b) TMP 10 mM.

for ^{3}**A**, new absorption bands appear in the transient spectra. These new absorptions were attributed to the radical anion **A**$^{-\bullet}$ of the respective oxoisoaporphine, because with these amines only single electron-transfer quenching of triplet oxoisoaporphine is possible, with no further reactions due to the lack of a transferable α-H; see Scheme 2. Triplet quenching constants, k_{ET}, vary from near the diffusion limit for DABCO with $k_{ET} = 4.3 \times 10^9$ to 2.5×10^7 M^{-1} s^{-1} for TMP.

Figure 5a show the transient spectra obtained for 2,3-dihydro-oxoisoaporphine, **A3**, in the presence of DABCO 0.1 mM. The spectra show a maximum at 485 nm attributed to the radical anion **A3**$^{-\bullet}$ and a shoulder at 465 nm that was attributed to DABCO$^{+\bullet}$ cation radical;[30] both absorptions decay with a lifetime of about 20 μs related to the back electron-transfer process, of the ion radical pair leading to the initial reactants, with a kinetic constant $k_{-ET} = 5 \times 10^4$ s^{-1} estimated from the absorption decay. The low value for this constant is consistent with spin-forbidden electron back transfer.[5,6] Similar results were obtained with TMP as the electron donor, but, due to the lower k_{ET} as compared with DABCO, we are able to observe the radical anion absorption at 485 nm and the triplet decay at 450 nm with lifetimes of 230 and 10 μs, respectively; see Figure 5b. Both transient spectra show the absorption band at 485 nm attributed to **A3**$^{-\bullet}$.

Flash photolysis of oxoisoaporphine **A3**, in the presence of excess of the non-hydrogen-donating amine triphenylamine, TPA, show the characteristic absorption of the radical cation, TPA$^{+\bullet}$, near 650 nm,[31] the sharp band with a maximum at 490 nm due to absorption of radical anion, and a broad band near 400 nm, whose absorbance increases with the amine concentration, Figure 6. Aromatic amines are known for their ability to form exciplexes;[32−34] thus absorption due to an exciplex with a considerable character of a charge-transfer complex cannot be disregarded, but the signal at 400 nm could be attributed to tetraphenylbenzidine whose formation from the reaction between TPA$^{+\bullet}$ and ground TPA or by dimerization of TPA$^{+\bullet}$ radical cation[35] has been reported in similar systems. Also is apparent a red shift in the maximum of the band at 490−500 nm that occurs at times longer than the maximum absorption of tetraphenylbenzidine, suggesting the formation of an adduct between the **A3**$^{-\bullet}$ radical cation and tetraphenylbenzidine. Molar absorptivity estimation of the radical anion **A3**$^{-\bullet}$ could be made

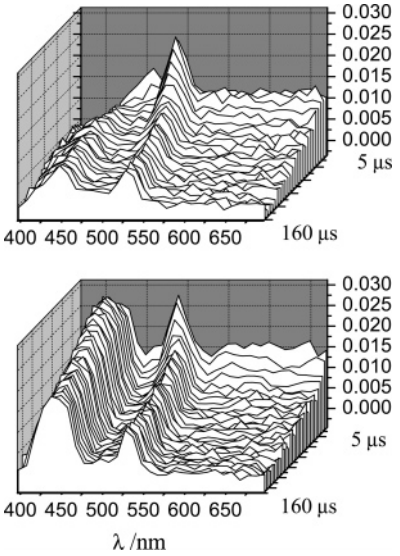

Figure 6. Evolution of the absorption spectra of 2,3-dihydro-oxoisoaporphine **A3** in the presence of 0.2 (upper) and 0.41 (lower) mM TPA.

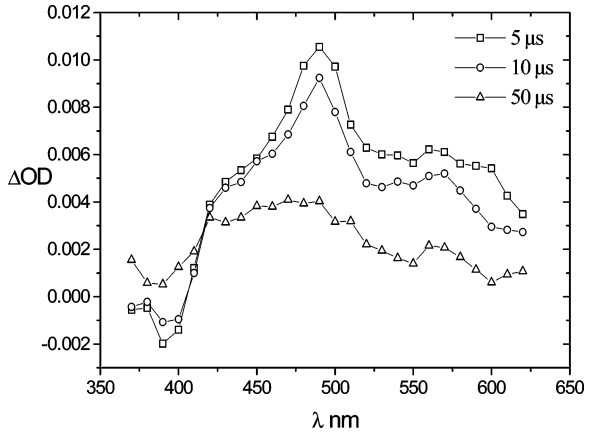

Figure 7. Transient spectra of 5-metoxi-2,3-dihidro-oxoisoaporphine in the presence of 6.4×10^{-4} M DABCO.

from the absorbance of $TPA^{+\bullet}$ and $\mathbf{A3}^{-\bullet}$ at 647 and 485 nm, respectively, by assuming a stoichiometric relationship between the ion radical species at short time after the laser pulse. From the reported $\epsilon = 1.3 \times 10^4$ M^{-1} cm^{-1}, at 647 nm[31] for $TPA^{+\bullet}$, an $\epsilon = 2.0 \times 10^4$ $M^{-1}c$ m^{-1} at 485 nm can be estimated for $\mathbf{A3}^{-\bullet}$.

The transient spectrum of the radical anion of 5-methoxy-2,3-dihydro-oxoisoaporphine $\mathbf{A2}^{-\bullet}$, obtained in the presence of DABCO 6.4×10^{-4} M, presents two maxima: at 490 and 570 nm and a shoulder at 430 nm that may be due to residual absorption of $DABCO^{+\bullet}$ radical cation.[30] The bands at 490 and 570 nm decay monoexponentially, with equal lifetime, indicating that they are absorptions of the same species $\mathbf{A2}^{-\bullet}$, decaying with a constant rate of 2×10^4 s^{-1}. In Figure 7, the spectra are shown at 5, 10, and 50 μs after the laser shot.

When hydrogen donating amines were used, the photoreduction continued with the formation of hydrogenated neutral radical **A-NH**$^{\bullet}$, that after the second electron transfer generates the metastable photoproduct **A-NH**$^{-}$ with more complex transient spectra due to the simultaneous absorption of the transients species. However, the previously identified absorption due to the triplet and to the radical anion of the oxoisoaporphine and the kinetic evolution of them allow the assignment of the neutral radical **A-NH**$^{\bullet}$ absorption.

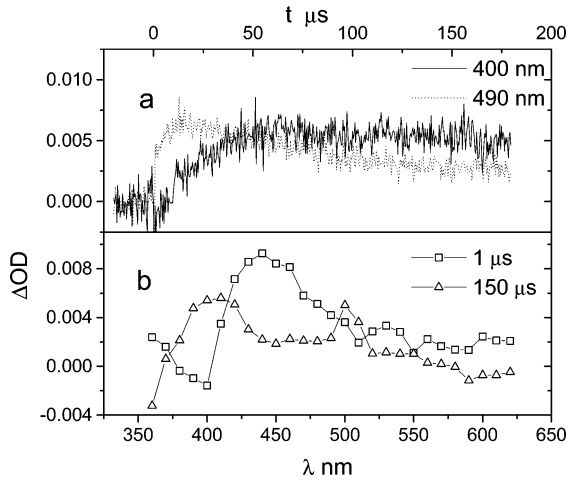

Figure 8. (a) Growth and decay curves for signals of radical anion $\mathbf{A3}^{-\bullet}$ (dot-line) and neutral N-hydrogen radical **A-NH**$^{\bullet}$ (solid-line) and (b) transient spectra of **A3** in the presence of [TEA] 2.39×10^{-5} M, 1.0 and 150 μs after the laser shot.

In the laser flash photolysis of oxoisoaporphine **A3**, in the presence of TEA, the three transients species could be observed on different time scales. First, at short time after the laser shot, the known triplet absorption, with maximum at 450 nm, appears. The radical anion with absorption maximum near 490 nm appears with a longer lifetime, together with growth of a new absorption band centered at 390 nm, Figure 8b. This new absorption could be attributed to the neutral N-hydrogen radical **A3-NH**$^{\bullet}$. The decay and growth, curves of Figure 8a, show that formation of radical anion $\mathbf{A3}^{-\bullet}$, monitored at 490 nm, occurs almost immediately after the laser shot; roughly 50% of their amplitude is reached in less than 1 μs, as expected for their electron-transfer rate, $k_{ET} = 6{,}7 \times 10^8$ M^{-1} s^{-1}, followed by a monoexponential rise, while the proton transfer from $TEA^{+\bullet}$ to $\mathbf{A3}^{-\bullet}$ occurs on a longer time scale as shown in Figure 8a where the growth and decay of the absorptions attributed to $\mathbf{A3}^{-\bullet}$ and **A3-NH**$^{\bullet}$ were shown. In the condition of the experiment, [TEA] $= 2.4 \times 10^{-5}$ M, the triplet decay with a $\tau = 10 \pm 1.8$ μs, that agrees with the growth time of radical anion $\mathbf{A3}^{-\bullet}$ at 490 nm, $\tau = 9.7 \pm 1.8$ μs, which decays with a rate constant of 1.6×10^4 s^{-1}, estimated from the lifetime of near 62 μs. From the growth time of the signal attributed to **A3-NH**$^{\bullet}$, at 400 nm, $\tau = 165 \pm 11$ μs, a rate constant for protonation of $\mathbf{A3}^{-\bullet}$, $k_{H+} = 6.1 \times 10^3$ s^{-1} was estimated by assuming that the radical ion pair stays in the solvent cage as suggested by the monoexponential decay of absorption assigned to the radical anion. However, the rate constant for decay of $\mathbf{A3}^{-\bullet}$ is 2.6 times greater than the rate constant of the proton transfer, which should be the rate-limiting step for the formation of the metastable photoproduct **A-NH**$^{-}$ reported previously.[8]

Similar results were obtained with tribenzylamine (data not shown) with the observation of absorption bands maxima slightly shifted to the red at 500 nm for the radical anion, $\mathbf{A3}^{-\bullet}$, and 415 nm for the N-hydrogen neutral radical, **A3-NH**$^{\bullet}$, with respect to TEA. The red shift could be attributed to interaction of the transient species with ground tribenzylamine.

With the two α-H donor amines, it was possible to observe the generation of the neutral radical **A3-NH**$^{\bullet}$ with a maximum of absorption near 400 nm in agreement with the PM3/ZINDO/S calculated spectra, that predicts the stronger transition at 362 nm for **A3-NH**$^{\bullet}$ and at 374 and 367 nm for **A1** and **A2** neutral radicals, respectively; see Table 2. The greater inconsistency between the experimental and calculated spectra is observed for **A3-NH**$^{\bullet}$ with an energy difference of ~0.33 eV, that could

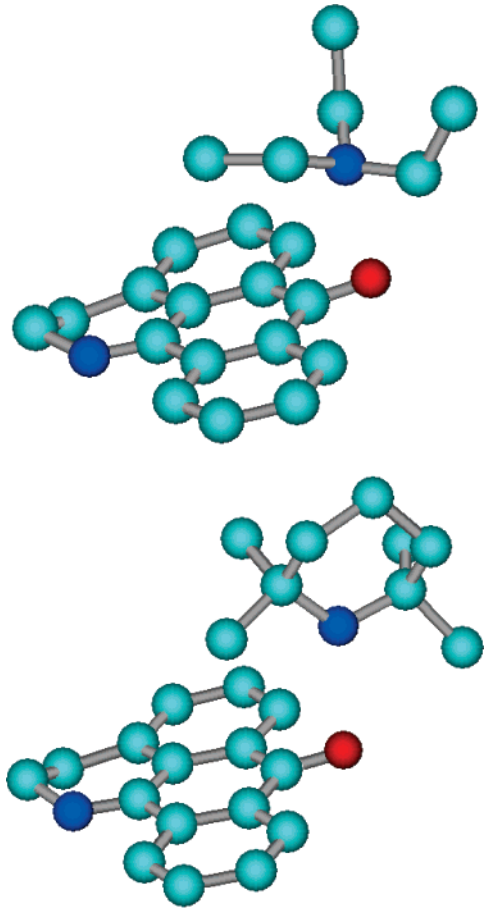

Figure 9. Conformation of ion radical pair for **A3**$^{-\bullet}$**/TEA**$^{+\bullet}$ and **A3**$^{-\bullet}$**/TMP**$^{+\bullet}$ systems; hydrogen atoms have been omitted for clarity.

be attributed to the approximations in the calculation method used, where only the isolated species were considered disregarding any solvent effect. Despite this, the experimental spectrum is well reproduced with respect to the wavelength of maximal absorption, and some transitions between 530 and 560 nm could be seen in the experimental spectra shown in Figures 5 and 6.

For all of the studied systems, an experimental transient absorption is observed near 490 nm irrespective of the oxoisoaporphine or the amine used. Because it appears in the presence of non α-H donating amines, where the only possible process is the photoinduced electron transfer, its was assigned to the respective radical anion **A**$^{-\bullet}$.

However, the ZINDO/S/PM3 spectral calculation made for the isolated oxoisoaporphine radical anion **A**$^{-\bullet}$ does not predict absorptions near 490 nm, where its appears, predicting the strongest transitions above 600 nm (transition not observed experimentally; see Table 2); therefore, the isolated radical anion could not be responsible for absorption at 490 nm.

A more realistic approach to calculation should consider the associated radical cation of the amine, formed in the photoinduced electron transfer, with the optimization of the whole molecular system. Optimizations of the molecular systems were made, first by a fully separated optimization of the oxoisoaporphine radical anion, **A**$^{-\bullet}$, and amine radical cation $R_3N^{+\bullet}$ at PM3 level, then both molecules were merged and fully optimized as a molecular system by using Molecular Mechanics method MM^+, followed by a single point triplet state ZINDO/S calculation to estimate the absorption spectra. Several optimizations with different initial locations for the amino nitrogen with respect to the oxoisoaporphine were made to find the most stable conformation for the molecular system, obtaining geometries

TABLE 3: ZINDO/S/MM$^+$ Calculated Spectra for the Ion Radical Pair A$^{-\bullet}$/Amine$^{+\bullet}$ for 2,3-Dihydro-oxoisoaporphine, A3; See Text

amine$^{+\bullet}$	DABCO	TMP	TEA
	1510.9 (0.013)	1515.7 (0.001)	1460.8 (0.035)
	1146.1 (0.011)	1389.0 (0.061)	1266.6 (0.036)
	624.6 (0.002)	799.2 (0.007)	1041.5 (0.017)
	483.6 (0.208)	588.0 (0.173)	575.6 (0.175)
λ nm (osc. strength)	453.6 (0.004)	449.8 (0.477)	449.7 (0.507)
	449.1 (0.047)	438.4 (0.173)	439.7 (0.082)
	340.2 (0.009)	370.2 (0.021)	337.3 (0.033)
		335.5 (0.056)	

similar to those shown in Figure 9 for **A3**$^{-\bullet}$**/TEA**$^{+\bullet}$ and **TMP**$^{+\bullet}$ systems, where the distances of amine N to O of C═O of the oxoisoaporphine vary between 2.4 and 2.6 Å. The calculated spectra for the systems formed by DABCO, TMP, and TEA radical cation and 2,3-dihydro-oxoisoaporphine radical anion, **A3**$^{-\bullet}$, are summarized in Table 3 and for **A1**$^{-\bullet}$ and **A2**$^{-\bullet}$ in Table 2S.

All of the considered systems, Table 3 and Table 2S, generate the strongest transition near the experimentally observed absorption maximum at 490 nm, suggesting that the absorbing species are the radical ion pairs and not the isolated radical anion of the oxoisoaporphines, validating also the estimation of a first-order back electron-transfer rate constant in the 10^4 s^{-1} range.

The same calculations were repeated by considering the singlet state of the former molecular systems obtaining active transitions at wavelength below 350 nm disregarding photoinduced electron transfer involving the excited singlet state of the oxoisoaporphines.

The good fit between the transient absorption at 490 nm and the calculated spectra of the ion radical pair permits us to conclude that the observed absorption should be attributed to the ion radical pair in triplet state or to a triplet exciplex with a great charge-transfer character, supporting our assumptions about the triplet nature of the photoreactive state.

These theoretical results support the reaction mechanism with the formation of a long-lived triplet ion radical pair that decays by the spin-forbidden back electron transfer in competition with the proton-transfer process as the probable rate-limiting step in the presence of α-H donating amines.

Conclusions

The triplet−triplet absorptions of the three studied oxoisoaporphines were characterized, next to the intermediate transients generated in the photoreduction of the oxoisoaporphines, that were generated with amines capable or not of donating α-H, making possible the assignment of the bands of absorption of the radical anion of the oxoisoaporphine to 490 nm and of the hydrogenated neutral radical to 390 nm. Semiempirical quantum mechanical calculations of the absorption spectra of the intermediates, calculated using ZINDO/S on the optimized PM3 geometry, reproduce the experimental spectra of the triplets and of the neutral hydrogenated radical. The calculated spectra for the isolated radical anion differ notably from the experimentally obtained ones, but when considering the radical cation of the amine, the calculated spectrum reproduces adequately that obtained experimentally, supporting the formation of a radical ion pair complex as the first step of photoreduction.

Semiempirical quantum mechanical methods used in this work allow us to conclude that the observed absorption at 490 nm should be attributed to the radical ion pair or to an exciplex, with a great character of charge-transfer complex, formed by

the oxoisoaporphine and the amine. These results show how a simple, rapid, and low demanding computing method provides good spectral results that permit us to assign absorption spectra to transient species.

The transient species detected in the present work support the stepwise mechanism of transfer of electron, proton, electron, previously proposed for the photoreduction of 2,3-dihydro-oxoisoaporphines.

Experimental Section

Acetonitrile, HPLC, or spectroscopic grade was used as received. Triethylamine, TEA, Aldrich, was stored over potassium hydroxide prior to vacuum distillation trap-to-trap, and 2,2,6,6-tetramethylpiperidine, TMP, Aldrich 99+%, was also vacuum distilled. Both amines were sealed into glass tubes at 10^{-4} Hg mm and stored at −18 °C. Before each experiment, a new tube was opened to ensure freshness of the amine.

DABCO, Aldrich, was used as received. DABCO solutions were prepared immediately before use. Triphenylamine, Aldrich 98%, was purified by recrystallization from methanol.

Synthesis of oxoisoaporphines A1, A2, and A3 was achieved by the procedure reported by Favre et al.[15] and by Walker et al.[16] and completely characterized as reported previously.[17]

Laser flash photolysis experiments were performed on the instrument described previously.[6,36] Optimal results were obtained with solutions with absorbance 0.6 at the excitation wavelength. Solutions (3 mL) of oxoisoaporphine, with absorbances between 0.2 and 0.6 at 355 nm, were purged with N_2 for 20 min in a 10 mm fluorescence quartz cell sealed with a septum. Immediately after purging, an aliquot of pure or diluted amine was added through the septum for the quenching or spectral experiments. Bimolecular rate constants were obtained from slopes of Stern−Volmer type plots of $1/\tau$ versus [quencher]. For decay of an ion-radical pair, first-order rate constants were estimated from the inverse of lifetime of the monoexponential decay of the respective absorptions.

Transient spectra in the presence of amines were monitored typically with not more than 4 laser pulses for each monitored wavelength. When flash photolysis was made in the presence of TEA, the integrities of solutions were assured by taking 10 min rest intervals between each wavelength measurement. Also, the UV spectra of solutions were checked after a few laser shots.

Triplet quantum yields for oxoisoaporphines were measured by energy transfer to β-carotene with benzophenone as standard. The measurements were made by monitoring the 520 nm ΔOD corresponding to β-carotene triplets[37] of solutions of oxoisoaporphine and benzophenone in acetonitrile, whose absorbances at 355 nm were matched approximately to 0.2. Aliquots of β-carotene in benzene were added to the former N_2 purged solutions to reach a plateau in the absorption signal at 520 nm, to ensure complete energy transfer to β-carotene. To the oxoisoaporphina solutions was added the same quantity of β-carotene, and ΔOD at 520 nm was measured attenuating the laser power with glass slides and measuring the impinging power with a pyroelectric power meter Quantel model MPI-310.

The triplet quantum yield was calculated from the slope of the plots of ΔOD_{520} versus laser power, measured with the oxoisoaporphine and benzophenone by using: $\Phi^T = (m_{oxo}/m_{bzph}) \times \Phi^T_{bzph}$, where m_{oxo} and m_{bzph} were the slopes of the optical densities of β-carotene triplet absorption at 520 nm sensitized, respectively, by oxoisoaporphine and benzophenone, and Φ^T_{bzph} is the triplet quantum yield of benzophenone[38] taken as 1.00. To be sure that no direct excitation of β-carotene takes place, a cell with pure purged acetonitrile was irradiated with the same aliquots used in the preceding experiments. In this cell, no absorption at 520 nm was observed, indicating no direct excitation of β-carotene. The integrities of the solutions were monitored by UV spectrophotometry, and no more than 4 laser pulses were used at each laser power. This procedure assumes an energy transfer yield of 100%.

Quantum mechanical calculations were made using a Windows version of HyperChem-6.01 by HyperCube, Inc. in a compatible personal computer with an Intel Pentium 4 processor of 2.0 GHz with 512 MB of RAM. The ZINDO/S IC calculations were made with 5 + 5 MO; by including more MO (10 + 10), a greater number of absorption lines in the high-energy region beyond the range of UV spectrometers were obtained, without affecting the spectrally interesting region. DFT-B3LYP/6-31G* calculations were made by using the Windows version of the Gaussian 03 suite of programs.[39]

Acknowledgment. We thank FONDECYT Grant No. 1030963 and Proyecto Facultad-CEPEDEQ for financial support, and Prof. A. Zanocco who made possible the use of the Gaussian software.

Supporting Information Available: Calculated and experimental spectra of **A1-NH**$^-$, and transient calculated spectra for methoxylated derivatives. This material is available free of charge via the Internet at http://pubs.acs.org.

References and Notes

(1) Gould, I. R.; Farid, S. *J. Am. Chem. Soc*. **1993**, *115*, 4814−4822.
(2) Ci, X.; da Silva, R. S.; Nicodem, D.; Whitten, D. G. *J. Am. Chem. Soc*. **1989**, *111*, 1337−1343.
(3) Gan, H.; Whitten, D. G. *J. Am. Chem. Soc*. **1993**, *115*, 8031−8037.
(4) Schanze, K. S.; Lee, L. Y. C.; Giannotti, C.; Whitten, D. G. *J. Am. Chem. Soc*. **1986**, *108*, 2646−2655.
(5) De la Fuente, J. R.; Cañete, A.; Zanocco, A. L.; Saitz, C.; Jullian, C. *J. Org. Chem*. **2000**, *65*, 7949−7958.
(6) De la Fuente, J. R.; Cañete, A.; Saitz, C.; Jullian, C. *J. Phys. Chem. A* **2002**, *106*, 7113−7120.
(7) Görner, H.; Döpp, D.; Dittmann, A. *J. Chem. Soc., Perkin Trans. 2* **2000**, 1723−1733.
(8) De la Fuente, J. R.; Jullian, C.; Saitz, C.; Sobarzo-Sánchez, E.; Neira, V.; González, C.; López, R.; Pessoa-Mahana, H. *Photochem. Photobiol. Sci*. **2004**, *3*, 194−199.
(9) De Laive, P. J.; Foreman, T. K.; Giannotti, C.; Whitten, D. G. *J. Am. Chem. Soc*. **1980**, *102*, 5627−5631.
(10) Kim, J. M.; Cho, I. S.; Mariano, P. S. *J. Org. Chem*. **1991**, *56*, 4943−4955.
(11) Sugimoto, Y.; Babiker, H. A. A.; Inanaga, S.; Kato, M.; Isogay, A. *Phytochemistry* **1999**, *52*, 1431−1435.
(12) Yu, B. W.; Meng, L. H.; Chen, J. Y.; Zhou, T. X.; Cheng, K. F.; Ding, J.; Qin, G. W. *J. Nat. Prod*. **2001**, *64*, 968−970.
(13) Hu, S.; Xu, S.; Yao, X.; Cui, C.; Tezuka, Y.; Kikuchi, T. *Chem. Pharm. Bull*. **1993**, *41*, 1866−1868.
(14) Hou, C.; Xue, H. *Acta Pharm. Sin*. **1985**, *20*, 112−117.
(15) Fabre, J. L.; Farge, D.; James, C. Dibenzo[de,h]quinoline derivatives, U.S. Patent No. 4,128,650, 1978.
(16) Walker, G. N.; Kempton, R. J. *J. Org. Chem*. **1971**, *36*, 1413−1416.
(17) Sobarzo-Sanchez, E. "Sintesis y Reactividad en el Ámbito de las 7H-Dibenzo(de-h)quinolinas", Tesis de Doctorado, Universidad de Chile, 2003.
(18) De la Fuente, J. R.; Jullian, C.; Saitz, C.; Neira, V.; Poblete, O.; Sobarzo-Sánchez, E. *J. Org. Chem.*, submitted.
(19) Gao, G.; Wei, C. C.; Jeevarajan, A. S.; Kispert, L. D. *J. Phys. Chem*. **1996**, *100*, 5362−5366.
(20) Hu, K.; Evans, D. H. *J. Phys. Chem*. **1996**, *100*, 3030−3036.
(21) Maya, E. M.; Garcia-Frutos, E. M.; Vazquez, P.; Torres, T.; Martin, G.; Rojo, G.; Agullo-Lopez, F.; Gonzalez-Jonte, R. H.; Ferro, V. R.; Garcia de la Vega, J. M.; Ledoux, I.; Zyss, J. *J. Phys Chem. A* **2003**, *107*, 2110−2117.
(22) Stewart, J. J. P. MOPAC: A Semiempirical Molecular Orbital Program. *J. Comput.-Aided Mol. Des*. **1990**, *4*, 1−105.

(23) Ridley, J. E.; Zerner, M. C. *Theor. Chim. Acta* **1973**, *32*, 111−134.

(24) Forber, C.; Kelusky, E. C.; Bunce, N. J.; Zerner, M. C. *J. Am. Chem. Soc.* **1985**, *107*, 5884−5890.

(25) Abbott, L. C.; Batchelor, S. N.; Oakes, J.; Lindsay Smith, J. R.; Moore, J. N. *J. Phys. Chem. A* **2004**, *108*, 10208−10218.

(26) Shi, X.; Platz, M. S. *J. Phys. Chem. A* **2004**, *108*, 4385−4390.

(27) Allinger, N. L. *J. Am. Chem. Soc.* **1977**, *99*, 8127−8134.

(28) LaChapelle, M.; Belletête, M.; Poulin, M.; Godbout, N.; Le Grand, F.; Héroux, A.; Brisse, F. *J. Phys. Chem.* **1991**, *95*, 9764−9772.

(29) Tomasi, J.; Persico, M. *Chem. Rev.* **1994**, *94*, 2027−2094.

(30) Dunn, D. A.; Schuster, D. I.; Bonneau, R. *J. Am. Chem. Soc*. **1985**, *107*, 2802−2804.

(31) Oyama, M.; Nozaki, K.; Okasaki, S. *Anal. Chem.* **1991**, *63*, 1387−1392.

(32) Lewis, F. D.; Cohen, B. E. *J. Phys. Chem.* **1994**, *98*, 10591−10597.

(33) Burkhart, R. D.; Jhon, N.-I. *J. Phys. Chem.* **1991**, *95*, 7189−7196.

(34) Kiyota, T.; Yamaji, M.; Shisuka, H. *J. Phys. Chem.* **1996**, *100*, 672−679.

(35) Oyama, M.; Higuchi, T.; Okasaki, S. *Electrochem. Solid State Lett.* **2002**, *5*, E1−E3.

(36) Viteri, G.; Edwards, A. M.; De la Fuente, J.; Silva, E. *Photochem. Photobiol*. **2003**, *77*, 535−540.

(37) Bensasson, R. V.; Dawe, E. A.; Long, D. A.; Land, E. J. *J. Chem. Soc., Faraday Trans. 1* **1977**, *73*, 1319−1325.

(38) Murov, S. L.; Carmichael, I.; Hug, G. L. *Handbook of Photochemistry*; Marcel Dekker: New York, 1993; Vol. 1, p 378.

(39) Frisch, M. J.; Trucks, G. W.; Schlegel, H. B.; Scuseria, G. E.; Robb, M. A.; Cheeseman, J. R.; Montgomery, J. A., Jr.; Vreven, T.; Kudin, K. N.; Burant, J. C.; Millam, J. M.; Iyengar, S. S.; Tomasi, J.; Barone, V.; Mennucci, B.; Cossi, M.; Scalmani, G.; Rega, N.; Petersson, G. A.; Nakatsuji, H.; Hada, M.; Ehara, M.; Toyota, K.; Fukuda, R.; Hasegawa, J.; Ishida, M.; Nakajima, T.; Honda, Y.; Kitao, O.; Nakai, H.; Klene, M.; Li, X.; Knox, J. E.; Hratchian, H. P.; Cross, J. B.; Bakken, V.; Adamo, C.; Jaramillo, J.; Gomperts, R.; Stratmann, R. E.; Yazyev, O.; Austin, A. J.; Cammi, R.; Pomelli, C.; Ochterski, J. W.; Ayala, P. Y.; Morokuma, K.; Voth, G. A.; Salvador, P.; Dannenberg, J. J.; Zakrzewski, V. G.; Dapprich, S.; Daniels, A. D.; Strain, M. C.; Farkas, O.; Malick, D. K.; Rabuck, A. D.; Raghavachari, K.; Foresman, J. B.; Ortiz, J. V.; Cui, Q.; Baboul, A. G.; Clifford, S.; Cioslowski, J.; Stefanov, B. B.; Liu, G.; Liashenko, A.; Piskorz, P.; Komaromi, I.; Martin, R. L.; Fox, D. J.; Keith, T.; Al-Laham, M. A.; Peng, C. Y.; Nanayakkara, A.; Challacombe, M.; Gill, P. M. W.; Johnson, B.; Chen, W.; Wong, M. W.; Gonzalez, C.; Pople, J. A. *Gaussian 03*, revision B.03; Gaussian, Inc.: Pittsburgh, PA, 2003.